

## Effect of methyl acetate on low-temperature performance of $\text{LiCo}_{1/3}\text{Ni}_{1/3}\text{Mn}_{1/3}\text{O}_2$ cathode and graphite anode

Hui Zhang<sup>1,a</sup>, Jiahui Chen<sup>1,b</sup> and Cuihua Li<sup>1,c,\*</sup>

<sup>1</sup> Department of Chemistry and Chemical Engineering, Shenzhen University, Shenzhen, China

<sup>a</sup>zhanghui2009love@126.com, <sup>b</sup>alivecjh@163.com, <sup>c</sup>licuihuasz@163.com

**Keywords:** Lithium ion battery, Low temperature performance, Methyl acetate,  $\text{LiCo}_{1/3}\text{Ni}_{1/3}\text{Mn}_{1/3}\text{O}_2$

**Abstract.**  $\text{Li}/\text{LiCo}_{1/3}\text{Ni}_{1/3}\text{Mn}_{1/3}\text{O}_2$  and  $\text{Li}/\text{graphite}$  half cells filled with methyl acetate (MA) with 1M  $\text{LiPF}_6$  function very well. Cells filled with 1 M  $\text{LiPF}_6$  in EC:DMC:EMC:MA(1:1:1:3) show good capacity retention  $147.5 \text{ mAh g}^{-1}$  after 50 cycles at  $25^\circ\text{C}$ . Electrochemical performance of Li-ion batteries is analyzed via the constant current charge-discharge test and cyclic voltammetry. It is found that adding a certain amount of MA improves the compatibility of electrolyte with electrodes. This study further shows that cells with 1M  $\text{LiPF}_6$  in EC:DMC:EMC:MA (1:1:1:3 v/v%) greatly improves the low-temperature performance in  $\text{LiCo}_{1/3}\text{Ni}_{1/3}\text{Mn}_{1/3}\text{O}_2$  cells. The capacity retention of the cell used this electrolyte is 92.2%, comparing to 86.8% of that without MA at  $-20^\circ\text{C}$ .

### Introduction

Nowadays, Li-ion batteries are a popular power source for many portable devices such as laptop computers, electric vehicles, and energy storage systems [1], due to their high energy density, high discharge voltage and long cycle life. However, cells with carbonate-only electrolytes always show notable capacity fading and voltage decline when they work at extremely low temperatures (for instance,  $-20^\circ\text{C}$ ) [2].

Several factors are known to contribute to the poor low temperature performance of Li-ion cells [3-5], including: (1) poor electrolyte conductivity. (2) poor lithium transport kinetics in the electrode materials. (3) slow diffusion and charge transfer at the electrolyte/electrode interphase. Of these factors, the electrolyte type selected has the most significant impact upon the low temperature of Li-ion cells. Solvent is the main element of electrolyte, whose nature is closely related to the performance of the electrolyte. The properties of electrolyte solvent including viscosity, dielectric constant, melting point, boiling point, flash point and oxidation reduction potential have great effect on electrochemical performance, safety performance and operating temperature of Li-ion cells. Most electrolytes for Li-ion cells use a mixture of ethylene carbonate (EC) and other linear organic carbonates such as diethyl carbonate (DEC) or ethyl methyl carbonate (EMC) with  $\text{LiPF}_6$  as the conductive salt. In these carbonate-based electrolytes, the presence of EC is normally necessary if graphite electrode is used [6]. However, the presence of EC increases the viscosity of the electrolytes, especially at low temperature.

In order to further lower the viscosity of EC-based electrolytes, co-solvents have been used. For instance, Smart et al. demonstrated that the use of low molecular weight organic esters in EC-based electrolytes greatly improved the electrolytes conductivity especially at low temperature [7-9]. Compared with common organic, linear carboxylic acid ester, methyl acetate, has low melting point ( $-98.7^\circ\text{C}$ ) and viscosity ( $0.33 \text{ mPa s}$ ). Adding a certain amount of methyl acetate could reduce the viscosity and melting point of the electrolysis system. This paper studied the electrolyte containing methyl acetate effects on low temperature electrochemical performance of Li-ion cells.

### Experimental

The  $\text{LiCo}_{1/3}\text{Ni}_{1/3}\text{Mn}_{1/3}\text{O}_2$  cathode and graphite anode materials were provided by Shenzhen Tiaojiao Co. Ltd. Battery grade Li salt ( $\text{LiPF}_6$ ) and carbonate solvents (EC, EMC and DMC) were provided by Shenzhen Optimum Nano Energy Co. Ltd. Methyl acetate (MA, >98%) was purchased

from J&K and used as received. Two different electrolytes were prepared for this study, including the following composition: *a*. 1 M LiPF<sub>6</sub> EC:DMC:EMC(1:1:1 v/v %); *b*. 1 M LiPF<sub>6</sub> EC:DMC:EMC:MA(1:1:1:3 v/v %). The cathode was prepared with a slurry composed of 80 wt% LiCo<sub>1/3</sub>Ni<sub>1/3</sub>Mn<sub>1/3</sub>O<sub>2</sub>, 10 wt% carbon black, and 10 wt% poly(vinylidene difluoride) binder in N-methyl pyrrolidone. The resulting slurry was cast on a circular Al foil with a diameter of 14 mm. All the electrodes were dried in vacuum at 110 °C for at least 12 h prior to use. The graphite anode was prepared by the same method of the cathode. The 2032-type coin cells with LiCo<sub>1/3</sub>Ni<sub>1/3</sub>Mn<sub>1/3</sub>O<sub>2</sub> cathode or graphite anode, Li foil, Celgard 2400 separator and the prepared electrolyte were assembled in Mbraun Ar-filled glove box.

Galvanostatic charge/discharge cycles of Li/LiCo<sub>1/3</sub>Ni<sub>1/3</sub>Mn<sub>1/3</sub>O<sub>2</sub> cells were conducted between 2.7 and 4.3 V on a CT2001A battery test system (Wuhan Land Electronics Co. Ltd, China). The cells were cycled with a constant rate of 0.2 C (1 C=155 mAh g<sup>-1</sup>) at room temperature (ca. 25 °C) and low temperature (-20 °C). The temperature was controlled with a constant temperature/humidity test chamber (Shenzhen Fuyida Equipment Co. Ltd, China). In order to reach full thermal equilibrium, the Li/LiCo<sub>1/3</sub>Ni<sub>1/3</sub>Mn<sub>1/3</sub>O<sub>2</sub> cells were soaked at the target temperature for 6 h and then determined the electrochemical performance. Li/graphite cells were also cycled galvanostatically with 0.2 C (1 C=372 mAh g<sup>-1</sup>) at room temperature. Cyclic voltammetry was performed on Solartron 1470E cell test system with a scan rate of 0.1 mV s<sup>-1</sup>.

## Results and discussion

Fig. 1 shows the initial charge-discharge curve of Li/LiCo<sub>1/3</sub>Ni<sub>1/3</sub>Mn<sub>1/3</sub>O<sub>2</sub> cells with electrolyte *a* and *b*. It can be seen that the discharge capacity for the cell with electrolyte *a* is 153.5 mAh g<sup>-1</sup>, corresponding to a coulombic efficiency of 84.7%. While for the cell with electrolyte *b* delivers a discharge capacity of 164.7 mAh g<sup>-1</sup> with a coulombic efficiency of 84.8%. The higher charge and discharge capacity of the cell using electrolyte *b* may be due to the addition of MA that lowers the viscosity of the electrolyte.

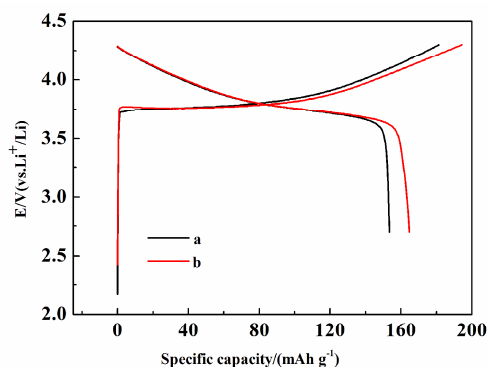


Fig. 1 Initial charge-discharge profiles of the Li/LiCo<sub>1/3</sub>Ni<sub>1/3</sub>Mn<sub>1/3</sub>O<sub>2</sub> cell using electrolyte (a) without MA and (b) with MA.

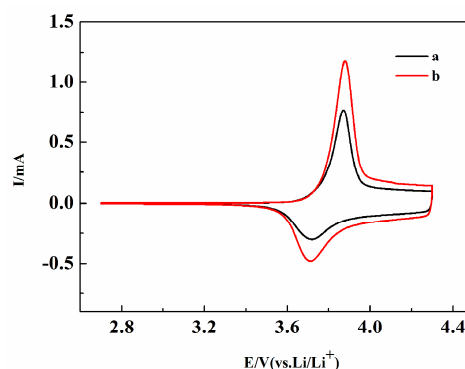


Fig. 2 Cyclic voltammograms of the Li/LiCo<sub>1/3</sub>Ni<sub>1/3</sub>Mn<sub>1/3</sub>O<sub>2</sub> cell using electrolyte (a) without MA and (b) with MA.

Cyclic voltammetry was carried out to understand the electrochemical behavior of LiCo<sub>1/3</sub>Ni<sub>1/3</sub>Mn<sub>1/3</sub>O<sub>2</sub> cathode in electrolytes with and without MA. As shown in Fig. 2, a broad anodic peak was observed at around 3.6-4.0 V, which can be attributed to the oxidation reaction between electrolyte and electrode. The redox current of the LiCo<sub>1/3</sub>Ni<sub>1/3</sub>Mn<sub>1/3</sub>O<sub>2</sub> cathode in electrolyte *b* is higher than that of electrolyte *a*, indicating faster kinetics of Li<sup>+</sup> (de)intercalation is achieved by the addition of MA. This result is in good agreement with the initial charge-discharge profiles.

Fig. 3 shows the cycling performance of Li/LiCo<sub>1/3</sub>Ni<sub>1/3</sub>Mn<sub>1/3</sub>O<sub>2</sub> cells with electrolyte *a* and *b* at 0.2 C and room temperature. These cells exhibit almost identical discharge capacity during cycling. The cell cycled in electrolyte *a* delivers initial discharge capacity of 150.3 mAh g<sup>-1</sup> and maintains 146.7 mAh g<sup>-1</sup> at the 50th cycle, corresponding to capacity retention of 97.6%. While for the cell

cycled in electrolyte *b*, slightly higher discharge capacity is achieved, delivering 147.5 mAh g<sup>-1</sup> after 50 cycles with capacity retention of 96.4%.

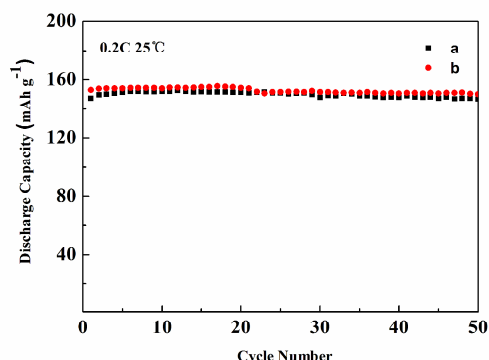


Fig. 3 Cycling performance of Li/LiCo<sub>1/3</sub>Ni<sub>1/3</sub>Mn<sub>1/3</sub>O<sub>2</sub> cells at room temperature: (a) without MA, (b) with MA.

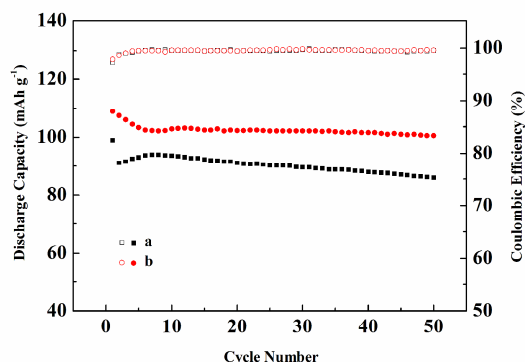


Fig. 4 Cycling performance of Li/LiCo<sub>1/3</sub>Ni<sub>1/3</sub>Mn<sub>1/3</sub>O<sub>2</sub> cells at -20° C: (a) without MA, (b) with MA.

Although, the cycling performance of the cell using electrolyte with and without MA is quite the same, great difference can be observed at -20 °C, as shown in Fig. 4. The cell without MA suffers capacity fading from 99 mAh g<sup>-1</sup> down to 86 mAh g<sup>-1</sup> with capacity retention of 86.8% after 50 cycles. In contrary, addition of MA results in capacity of 100.5 mAh g<sup>-1</sup> at 50th cycle and remains 92.2% of its initial capacity (109 mAh g<sup>-1</sup>). This suggests that MA can improve the cycling performance at low temperature. The MA, which has a very low melting point, significantly decreases the freezing temperature of the electrolyte, enabling Li<sup>+</sup> removal/insertion from/into the LiCo<sub>1/3</sub>Ni<sub>1/3</sub>Mn<sub>1/3</sub>O<sub>2</sub> electrode. In addition, the coulombic efficiencies of these cells are almost overlapped.

To verify the influence of MA on the graphite anode, galvanostatic cycle of Li/graphite cells with electrolyte *a* and electrolyte *b* was performed at 0.2 C and room temperature. The initial charge-discharge profiles are given in Fig. 5. It can be seen that there is no distinct difference between these two electrolytes except the small discharge plateau around 0.3 V. All cells deliver similarly high charge and discharge capacity of about 425 mAh g<sup>-1</sup> and 400 mAh g<sup>-1</sup> respectively. The initial over discharge capacity is due to the electrolyte reduction on the anode surface, which is involved in the build-up of solid/electrolyte interphase (SEI) film. This result indicates that the electrolyte with and with MA show good compatibility to the graphite anode.

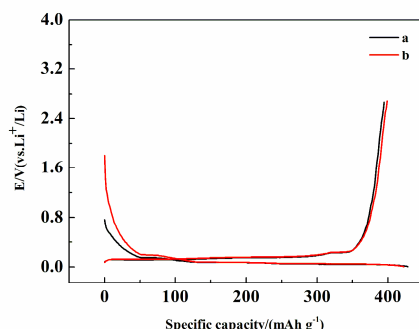


Fig. 5 Initial charge-discharge curves of the Li/graphite cell using electrolyte: (a) without MA and (b) with MA.

Fig. 6 compares the cyclic voltammograms of graphite anode in electrolyte *a* and *b* at a scan rate of 0.1 mV s<sup>-1</sup>. As can be seen, a reduction peak appears at around 0.6 V, which is attributed to the reduction of electrolyte solvents, resulting in the formation of SEI film on graphite surface. The peak located at around 0.01-0.3 V is due to the Li<sup>+</sup> intercalation and deintercalation. This peak remains much more stable in the cell using electrolyte *b*. Moreover, the current detected in the cell with MA is

remarkable higher than that without MA. These results suggest that highly reversible  $\text{Li}^+$  (de)intercalation process is supported by MA.

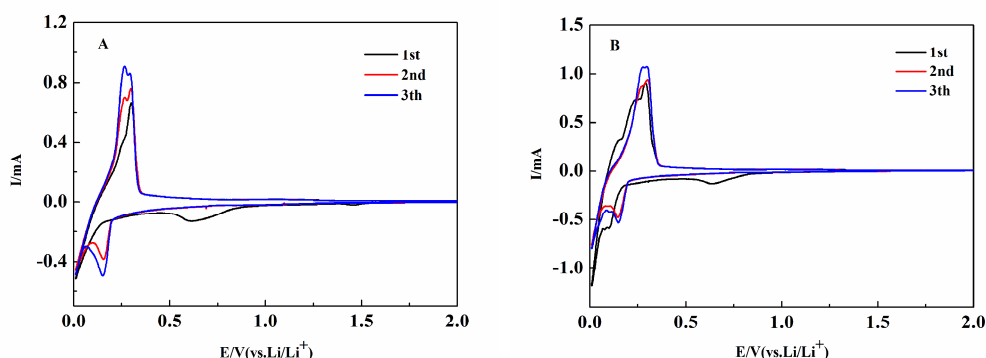


Fig. 6 Cyclic voltammograms of the Li/graphite cell using electrolyte: (a) without MA and (b) with MA.

## Conclusion

Li/LiCo<sub>1/3</sub>Ni<sub>1/3</sub>Mn<sub>1/3</sub>O<sub>2</sub> and Li/graphite half cells in the electrolyte filled with methyl acetate (MA) exhibit improved electrochemical performance at room and low temperature. Incorporation of MA improved the discharge capacity retention of Li/LiCo<sub>1/3</sub>Ni<sub>1/3</sub>Mn<sub>1/3</sub>O<sub>2</sub> cell from 86.8% to 92.2% after 50 cycles at -20°C. Moreover, better intercalation/deintercalation of  $\text{Li}^+$  into/out LiCo<sub>1/3</sub>Ni<sub>1/3</sub>Mn<sub>1/3</sub>O<sub>2</sub> cathode and graphite anode was achieved in the electrolyte with MA. These positive effects were ascribed to the intrinsic characteristic of MA, i.e. its low melting point and viscosity.

## Acknowledgement

This work was financially supported by Scientific and Technological Research and Development Foundation of Shenzhen City (JCYJ20140418193546111), 973 National Defense Project (613142020201) and Shenzhen Key Laboratory of Functional Polymer Foundation (FP20140008).

## References

- [1] B. Scrosati, J. Hassoun, Y.K. Sun, *Energy Environ. Sci.* 4 (2011) 3287-3295.
- [2] J. Li, C.F. Yuan, Z.H. Guo, Z.A. Zhang, Y.Q. Lai, J. Liu, *Electrochim. Acta* 59 (2012) 69-74.
- [3] G. Park, N. Gunawardhana, H. Nakamura, Y.-S. Lee, M. Yoshio, *J. Power Sources* 199 (2012) 293-299.
- [4] M. Petzl, M. Kasper, M.A. Danzer, *J. Power Sources* 275 (2015) 799-807.
- [5] F. Wang, J. Chen, Z. Tan, M. Wu, B. Yi, W. Su, Z. Wei, S. Liu, *J. Taiwan Inst. Chem. Eng.* 45 (2014) 1321-1330.
- [6] R. Petibon, J. Harlow, D.B. Le, J.R. Dahn, *Electrochim. Acta* 154 (2015) 227-234.
- [7] M.C. Smart, B.V. Ratnakumar, L.D. Whitcanack, K.B. Chin, S. Surampudi, H. Croft, D. Tice, R. Staniewicz, *J. Power Sources* 119-121 (2003) 349-358.
- [8] M.C. Smart, J.F. Whitacre, B.V. Ratnakumar, K. Amine, *J. Power Sources* 168 (2007) 501-508.
- [9] M.C. Smart, B.V. Ratnakumar, K.B. Chin, L.D. Whitcanack, *J. Electrochem. Soc.* 157 (2010) A1361-A13674.